

Article

Drought Monitoring Using Moderate Resolution Imaging Spectroradiometer-Derived NDVI Anomalies in Northern Algeria from 2011 to 2022

Ramzi Benhizia ^{1,*} , Kwanele Phinzi ² , Fatemeh Hateffard ³ , Haithem Aib ⁴  and György Szabó ¹ 

¹ Department of Landscape Protection and Environmental Geography, University of Debrecen, Egyetem tér 1, 4032 Debrecen, Hungary; szabo.gyorgy@science.unideb.hu

² Department of Geography and Environmental Studies, University of Zululand, KwaDlangezwa 3886, South Africa; phinzi@unizulu.ac.za

³ Department of Physical Geography, University of Stockholm, 10691 Stockholm, Sweden; hateffnegar@gmail.com

⁴ Department Biology and Environmental Sciences, University of Debrecen, Egyetem tér 1, 4032 Debrecen, Hungary; haithem.aib@eng.unideb.hu

* Correspondence: benhizia.ramzi@science.unideb.hu

Abstract: Drought has emerged as a major challenge to global food and water security, and is particularly pronounced for Algeria, which frequently grapples with water shortages. This paper sought to monitor and assess the temporal and spatial distribution of drought severity across northern Algeria (excluding the Sahara) during the growing season from 2011 to 2022, while exploring the relationship between the normalized difference vegetation index (NDVI) anomaly and climate variables (rainfall and temperature). Temporal NDVI data from the Terra moderate resolution imaging spectroradiometer (MODIS) satellite covering the period 2000–2022 and climate data from the European Reanalysis 5th Generation (ERA5) datasets collected during the period 1990–2022 were used. The results showed that a considerable portion of northern Algeria has suffered from droughts of varying degrees of severity during the study period. The years 2022, 2021, 2016, and 2018 were the hardest hit, with 76%, 71%, 66%, and 60% of the area, respectively, experiencing drought conditions. While the relationship between the NDVI anomaly and the climatic factors showed variability across the different years, the steady decrease in vegetation health indicated by the NDVI anomaly corroborates the observed increase in drought intensity during the study period. We conclude that the MODIS-NDVI product offers a cost-efficient approach to monitor drought in data-scarce regions like Algeria, presenting a viable alternative to conventional climate-based drought indices, while serving as an initial step towards formulating drought mitigation plans.

Keywords: drought; MODIS-NDVI; NDVI anomaly; remote sensing



Citation: Benhizia, R.; Phinzi, K.; Hateffard, F.; Aib, H.; Szabó, G. Drought Monitoring Using Moderate Resolution Imaging Spectroradiometer-Derived NDVI Anomalies in Northern Algeria from 2011 to 2022. *Environments* **2024**, *11*, 95. <https://doi.org/10.3390/environments11050095>

Academic Editors: Guobin Fu and Jason Levy

Received: 31 January 2024

Revised: 28 April 2024

Accepted: 30 April 2024

Published: 4 May 2024



Copyright: © 2024 by the authors. Licensee MDPI, Basel, Switzerland. This article is an open access article distributed under the terms and conditions of the Creative Commons Attribution (CC BY) license (<https://creativecommons.org/licenses/by/4.0/>).

1. Introduction

Water insecurity is a growing global concern, driven by factors such as climate change, population growth, and the demands of agriculture, energy, and industry [1–5]. Among various natural disasters, drought stands out as one of the most costly and widespread [3,4,6–8], exacerbating water scarcity and posing significant challenges. Drought, characterized by prolonged periods of below-normal precipitation, has far-reaching impacts on the environment, society, and economy [9]. Consequently, drought has attracted the attention of many scientists from a broad range of disciplines, such as environmental science, ecology, hydrology, meteorology, geology, and agriculture [10,11]. Drought occurs in all climatic regions, including humid, sub-humid, semi-arid, and arid climates [9,12,13], affecting both developed and developing societies [14]. Already, in developing continents such as Africa, which are largely dependent on agriculture, drought has had severe consequences, producing starvation and degradation [15–17].

The Mediterranean region, particularly the northern part of the African continent, is susceptible to drought conditions, primarily attributed to its pronounced climate change occurring at a rate surpassing that of the global average [18]. Several climate studies have shown that drought has affected most Mediterranean countries [19–23], including Algeria, which is the largest country in the Mediterranean region and Africa. Algeria is renowned for its long-term droughts, which have caused water scarcity and harmed the natural environment and human life in many parts of the country [6,7,24–30]. In recent decades, Algeria has experienced two significant drought episodes. The first occurred from 1943 to 1948, followed by a subsequent onset beginning in 1980. Notably, during the 1980s and 1990s, the central and western regions of Algeria faced a pronounced deficiency in rainfall, estimated at approximately 30%, while the eastern region also encountered a deficit of around 30% [31].

As the early detection of drought is critical for proactive decision making and preparation [32], many indices have been developed to monitor and quantify drought, such as the Palmer drought severity index (PDSI) [33], the standardized precipitation evapotranspiration index (SPEI) [34], and the standardized precipitation index (SPI) [35]. Although these indices are widely used around the world [36–43], they are based on meteorological data, such as precipitation and temperature, that may not be available promptly [44]. Furthermore, meteorological observations often have different record lengths and variable data quality [32,45], making it challenging to conduct consistent drought analysis [46].

Remote sensing data have been frequently used in recent years to measure drought at a minimal cost [44,47–50], mainly in areas where meteorological station measurements are unavailable [51]. Many drought indicators can be derived from remotely sensed data, such as the normalized difference vegetation index (NDVI), the vegetation condition index (VCI), the temperature condition index (TCI), and the vegetation health index (VHI), which have been used for drought detection and monitoring around the world [38,42,43,52–55]. Drought-prone regions can be identified using these vegetation indices, which assume that dryness reduces the photosynthetic capacity of terrestrial plants during the growing season [53–56]. Among these drought indices, the NDVI is widely used because it reflects the health of the vegetation by measuring factors such as the leaf area index (LAI) and net primary productivity [57,58]. However, NDVI reflectance can be negatively influenced by soil moisture and surface conditions, which are not easy to eliminate. Additionally, due to the significant time lag associated with the NDVI, rainfall, and temperature, the NDVI anomaly may be considered a more reliable drought metric than the NDVI [59–61]. It represents the difference between the average NDVI for a specific period in a given year and the corresponding average NDVI for the same period across multiple years [48,60,62]. Although remote-sensing-derived drought indices like the NDVI anomaly are commonly used for drought assessment [44,63,64], there has not been any research employing this method specifically for drought monitoring in Algeria. In general, prior drought studies in Algeria have mainly employed either the PDSI, the SPEI, or the SPI, focusing mainly on the north-western part of the country [65–67] or on individual watersheds [68–72]. Only one recent study [73] has delved into drought patterns and their effects on vegetation across North and West Africa between 2002 and 2018. However, this study lacked a focused analysis of Algeria, particularly since 2011, leaving a gap in our understanding of the specific geographical and temporal patterns of drought in northern Algeria. Recently, [74] assessed and characterized drought in northern Algeria, shedding light on the drought patterns within the region. This study, however, relied on climatic drought indices, with limited observations until 2015. Consequently, a study reflecting the more recent evolution of the drought patterns in northern Algeria is required.

Previous studies have analyzed the spatiotemporal patterns of drought in the region using remote sensing data, but these assessments have been limited to smaller geographic areas, focusing on specific parts of the region [75]. This limitation persists despite the capability of remote sensing to cover larger areas, because such drought assessments combine remote sensing with traditional climatic indices that require reliable rainfall data.

Unfortunately, the coverage of operational weather stations across most African countries, including Algeria, is sparse, with significant spatial gaps, and the data from individual stations are often incomplete [76]. For these reasons, and recognizing the need for detailed insights, especially across broader geographic regions like Algeria, this study aimed to examine the extent and severity of drought in northern Algeria from 2011 to 2022. The main objectives were to understand the drought's variation during the growing seasons over these years and to analyze the annual relationship between the vegetation (measured using the NDVI) and the climate over the twelve-year period. To the best of our knowledge, no previous study has covered such a large-scale assessment of the drought conditions in northern Algeria during the studied period using similar methodologies.

2. Materials and Methods

2.1. Study Area

Algeria, the largest country in Africa, spans an area of approximately 2,381,741 km². Situated in the northern section of the continent, the country stretches between 28.0339° N and 1.6596° E (Figure 1). Geographically, the country can be divided into two distinct regions, namely the northern and southern regions. The north, lying between the Mediterranean and the Sahara, boasts mountains, valleys, and plateaus. Here, the Tell Atlas and the Saharan Atlas, which are two significant mountain ranges, run east to west, separated by the High Plateau. The vast majority (about 80%) of Algeria is in the southern region, which is predominantly desert with no agricultural activity. Our study, however, focused on the northern region of Algeria, encompassing 375,815 km² or 15.77% of the country, and home to 40 provinces.

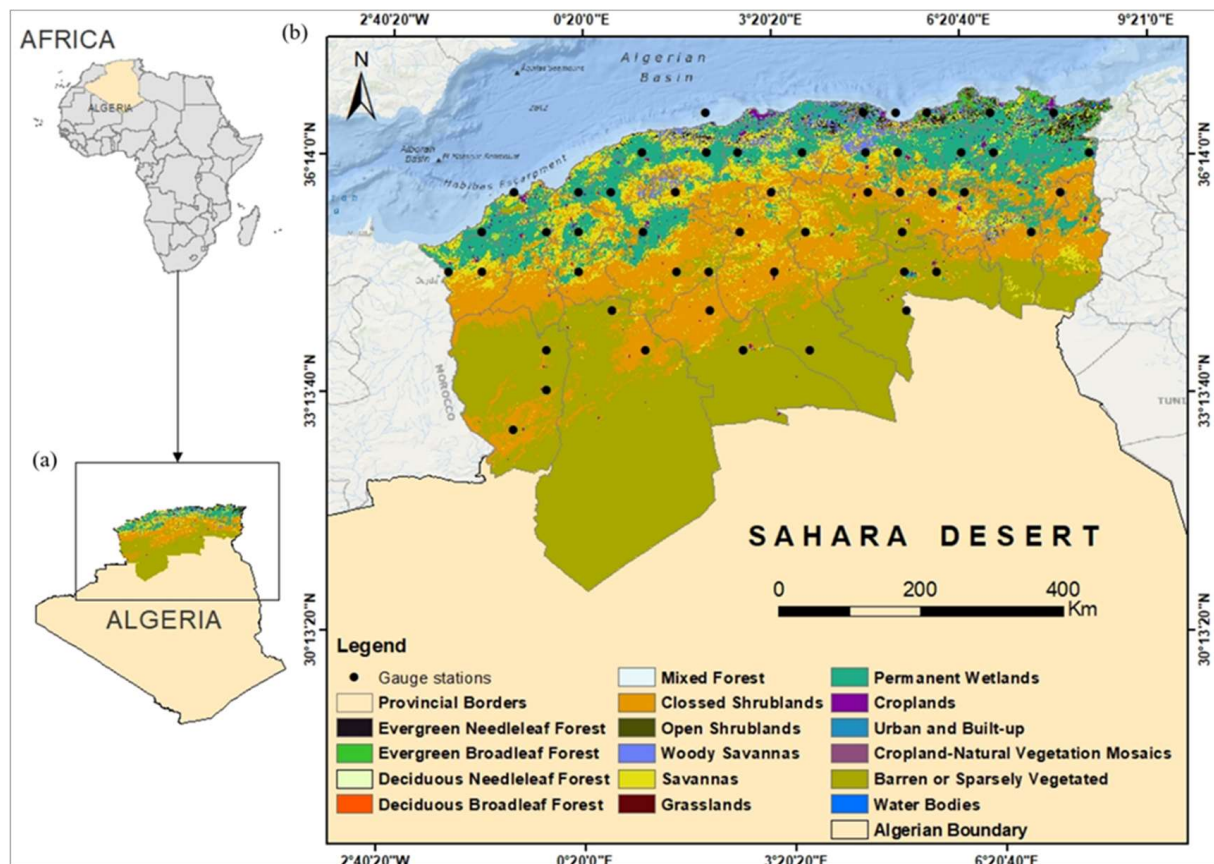


Figure 1. Location of the study area in northern Algeria (a). Land cover map of the northern part of Algeria and the location of weather stations falling within the study area (b).

The elevation of the study area varies from -36 m to 2301 m. This area exhibits three distinct climate zones, progressing from north to south, as identified in [77,78], as follows: (i) a Mediterranean climate marked by dry summers and mild, rainy winters; (ii) a sub-humid climate with relatively cool winters and occasional frost risks; and (iii) a semi-arid climate featuring cool winters and notably warm summers, with temperatures averaging 27°C during the peak months, such as July. Rainfall fluctuates considerably, with annual averages ranging from 100 to 800 mm. Notably, there are considerable variations in rainfall distribution between the northern and southern parts and between the eastern and western zones of the study area [27].

2.2. Data Collection and Processing

The satellite data utilized in this study consisted of two scenes of moderate resolution imaging spectroradiometer (MODIS) images covering the study area. These images were obtained free of charge from the National Aeronautics and Space Administration (NASA) through their Earthdata platform (<https://urs.earthdata.nasa.gov/>; accessed on 20 January 2023). More specifically, we obtained the MOD13Q1 v061 NDVI products with a 16-day temporal resolution and a spatial resolution of 250 m. The MODIS instrument is integral to the Earth Observing System (EOS), deployed on both the Terra and Aqua satellites. Launched in December 1999 and May 2002, respectively, these satellites serve as the host platforms for MODIS, a sophisticated 36-band imaging radiometer. Operating within a spatial resolution spectrum ranging from 250 m to 1 km, MODIS assumes a pivotal role in diverse scientific domains, including agriculture, forestry, meteorology, and urban studies. Its extensive deployment underscores its global significance in advancing research and applications across these multidisciplinary fields; in addition, these MODIS-NDVI data were acquired for each year's growing season (November–June), spanning over 23 years from 2000 to 2022. Additionally, monthly rainfall and temperature data from 1990 to 2022 were acquired for the research region. We used the ERA5 “European Reanalysis 5th Generation” dataset, produced by the European Centre for Medium-Range Weather Forecasts (ECMWF) [79]. Reanalyses are the result of decades of research into data assimilation methodologies, dynamical Earth system models, and investment in Earth observation. These products employ data assimilation to optimally combine various surface and satellite observations with a dynamical model, generating a self-consistent dataset that includes all essential climate variables from January 1940 to the present [79,80]. The ERA5 dataset offers insights into both observational uncertainty (integrated into the data assimilation framework) and stochastic uncertainty from the dynamical models. Furthermore, the ERA5 data were acquired in a gridded format, with a resolution of 0.25 degrees [79]. We utilized the KrigR package [81] to obtain ERA5 climate reanalysis data customized to our research area and time range. Furthermore, we used the Kriging interpolation from the KrigR package to perform the spatial downscaling of climatic variables to a resolution of 250 m.

2.3. Calculation of NDVI, Rainfall, and Temperature Anomalies

Through quantifying the vegetation density and chlorophyll content, the NDVI serves as a proxy for overall vegetation health [82], enabling a direct estimation of drought conditions. One way to determine notable drought indicators is the NDVI anomaly, which, in our context, is the difference between the long-term mean NDVI for a specific season and the mean NDVI for that same season across a different number of years. We employed a straightforward pixel-based method to determine NDVI anomalies where the long-term mean NDVI values were compared to the NDVI values in a specific year [83]. A positive NDVI variation indicates normal conditions, whereas negative values suggest severe drought conditions [44,84]

Before determining the NDVI anomaly, we took two preliminary steps. Firstly, we determined the mean NDVI during the growing season (from November to June) for each year, using the following formula (Equation (1)):

$$NDVI_{mean_i} = (NDVI_1 + NDVI_2 + NDVI_n) / n \tag{1}$$

where $NDVI_{mean}$ = mean NDVI value of the growing season in each i year; $NDVI_1$ = first NDVI month (November); and $NDVI_n$ = last NDVI month (June) in the growing season of i year. Secondly, we computed the long-term mean NDVI based on the following formula (Equation (2)):

$$\overline{NDVI} = \sum_{i=1}^n \frac{NDVI_{mean_i}}{n} \tag{2}$$

where \overline{NDVI} = long-term NDVI mean; and n = number of years considered for calculating the long-term mean, equal to the first 11 years (2000–2010) of the entire study period (2000–2022). We then calculated the NDVI anomaly for each growing season of the remaining twelve years (2011–2022), using the following formula (Equation (3)):

$$NDVI_{anomaly_i} = \frac{NDVI_{mean_i} - \overline{NDVI}}{\overline{NDVI}} \times 100 \tag{3}$$

where $NDVI_{anomaly_i}$ = NDVI anomaly for the growing season of the i year.

In addition to NDVI anomalies, we also determined anomalies for rainfall and temperature (Table 1). A 30-year long-term average spanning from 1990 to 2020 was calculated for these climatic variables, following the recommendation of the World Meteorological Organization (WMO) [85]. To ensure uniformity, rainfall and temperature anomalies were computed for the identical time frame (2011–2022) as that of the NDVI anomaly.

Table 1. Rainfall and temperature anomaly calculation, where EN refers to equation numbers.

Climate Variable	Equation	EN	Description
Rainfall	$Rf_{mean_i} = (Rf_1 + Rf_2 + Rf_n) / n$	(4)	Rf_{mean} = mean rainfall value of the growing season in each i year; Rf_1 = first month of the growing season; Rf_n = last month of the growing season in the i year.
	$\overline{Rf} = \sum_{i=1}^n \frac{Rf_{mean_i}}{n}$	(5)	\overline{Rf} = long-term mean rainfall; n = number of years considered for calculating the long-term mean, equal to 30 years (1990–2020).
	$Rf_{anomaly_i} = Rf_{mean_i} - \overline{Rf}$	(6)	$Rf_{anomaly_i}$ = rainfall anomaly for the growing season of the i year.
Temperature	$Tem_{mean_i} = (Tem_1 + Tem_2 + Tem_n) / n$	(7)	Tem_{mean} = mean temperature value of the growing season in each i year; Tem_1 = the first month of the growing season; Tem_n = last month of the growing season in the i year.
	$\overline{Tem} = \sum_{i=1}^n \frac{Tem_{mean_i}}{n}$	(8)	\overline{Tem} = long-term mean temperature; n = number of years considered for calculating the long-term mean, equal to 30 years (1990–2020).
	$Tem_{anomaly_i} = Tem_{mean_i} - \overline{Tem}$	(9)	$Tem_{anomaly_i}$ = temperature anomaly for the growing season of the i year.

2.4. Drought Severity Classification

The drought severity levels were determined by reclassifying the map of the NDVI anomaly into the following five categories: non-drought, slight drought, moderate drought, severe drought, and very severe drought (Table 2). This approach is widely recognized and has been used in drought severity assessments worldwide [44,84,86,87]. To analyze the

spatiotemporal patterns and variability, we examined the percentages of each drought level in a specific year within the study area. We used the ggplot2 package [88] in R software to graphically show the proportion of the area affected by drought in each year.

Table 2. The drought classification scheme used in this study.

Drought Class	Non-Drought	Slight Drought	Moderate Drought	Severe Drought	Very Severe Drought
NDVI anomaly (%)	Above 0	0 to −10	−10 to −25	−25 to −50	Below −50

2.5. Statistical Analysis of the Relationship between NDVI and Climate Anomalies

We employed ArcMap to generate a random sample of 988 points from which we retrieved the NDVI, rainfall, and temperature anomaly pixel values for each year. Considering the vast geographic extent of the study area, with over 6.9 million pixels, we specifically chose 988 pixels to facilitate clear and simple statistical interpretation. The Spearman correlation coefficient was then utilized to examine the relationship between the NDVI and climatic factors [44,86,87]. Unlike the Pearson correlation, the Spearman correlation does not assume a linear relationship between variables or a normal distribution of data [89,90]. For this reason, the Spearman correlation was chosen for this study because of the non-linear relationship between the NDVI and climatic variables. Based on the correlation values, the relationship between the NDVI and the climatic factors was classified into different levels, ranging from a negligible to a very strong correlation (Table 3). We used the R software [91] for computing the Spearman correlation coefficients and Microsoft Excel for plotting the NDVI and climate anomalies graph. To produce the NDVI–climate anomalies graph, we calculated the average anomaly from 988 pixels for each year.

Table 3. Correlation coefficient values and their associated interpretations [92].

Correlation Coefficient (+/−)	Interpretation
0.00–0.10	Negligible correlation
0.10–0.39	Weak correlation
0.40–0.69	Moderate correlation
0.70–0.89	Strong correlation
0.90–1.00	Very strong correlation

3. Results

3.1. Spatial and Temporal Changes in Seasonal NDVI from 2011 to 2022

The northern section of the region, notably the coastal provinces of Skikda, Tizi-Ouzou, Jijel, Annaba, El Tarf, Béjaïa, Tipaza, and Algiers, had higher NDVI values than the southern section, which encompasses a large percentage of the study area (Figure 2). The year 2013 had the highest maximum NDVI value (0.95), and the maximum NDVI value for all of the other years varied from 0.87 to 0.94. We also analyzed the distribution of NDVI values from 2011 to 2022 against the long-term NDVI (2000–2010) (Figure 3). The boxplots were consistently right-skewed, indicating the predominance of low NDVI pixel values. The median NDVI values across all years consistently fell below 0.25. Most years demonstrated a relatively stable NDVI value distribution, with notable exceptions in 2013, 2018, and 2022, where the medians were higher than the long-term NDVI.

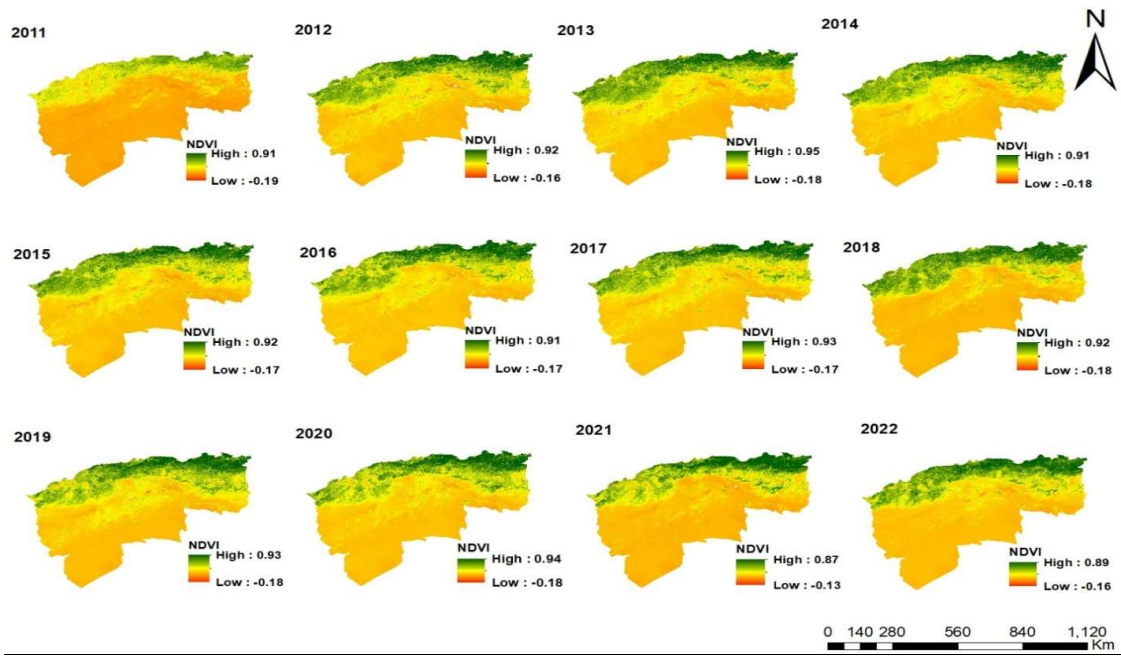


Figure 2. Spatial distribution of the mean NDVI for each year's growing season from 2011 to 2022.

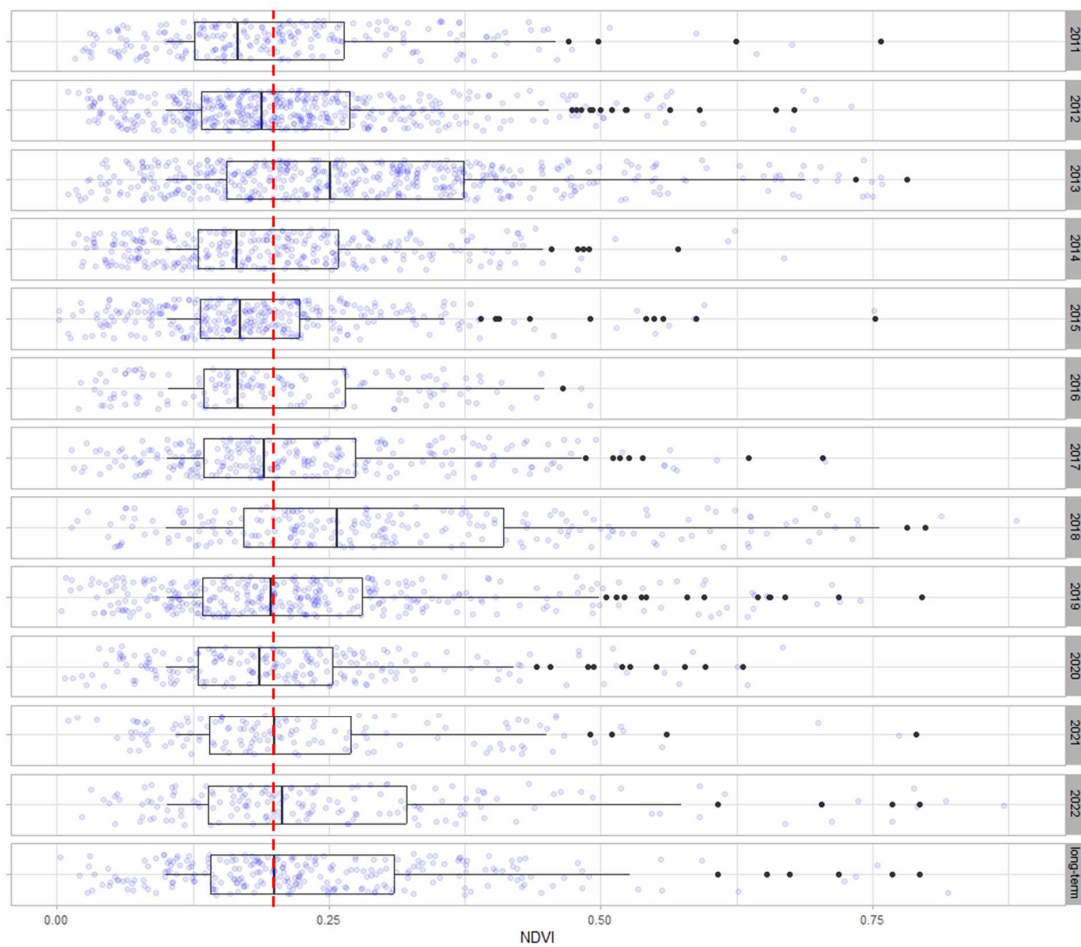


Figure 3. Temporal variation in seasonal mean NDVI from 2011 to 2022 compared to the long-term NDVI (the red dashed line denotes a long-term median NDVI value).

3.2. Drought Severity Assessment

The results revealed substantial temporal variability in the occurrence of drought throughout the study period (Figure 4). Among the years examined, 2012 and 2013 were the least drought-affected years, with the highest percentages (>70%) of non-drought conditions. On the contrary, the years 2016, 2021, and 2022 stood out as those most severely impacted by drought in northern Algeria. In 2016, around 39.93% of the region experienced slight drought, while 20.7% faced moderate drought conditions. A notable 5.79% of the area was affected by severe drought, reflecting a significant decline in vegetation health and increased water scarcity. Similarly, in 2021, the severity of drought escalated further, with 11.06% of the region being affected by severe drought conditions. However, it was in 2022 that the severity of drought reached a critical level, as only 23.92% of the region was classified as non-drought, while a substantial 76.08% of the area experienced slight drought to severe drought conditions, making it one of the most drought-affected years during the study period.

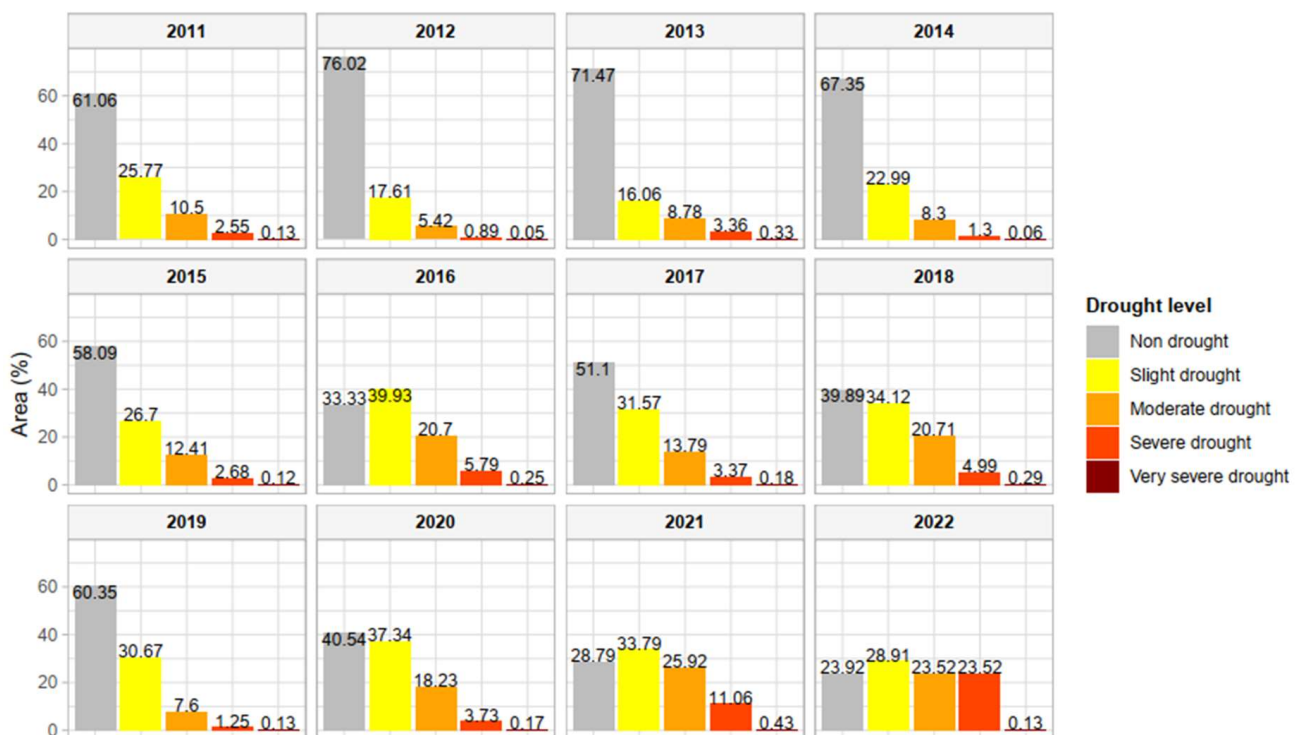


Figure 4. Percentage surface area of drought in northern Algeria from 2011 to 2022.

The western and central sections experienced more drought in 2011, while the eastern and south-eastern regions were mainly affected by drought in 2013 and 2017 (Figure 5). Similarly, in 2018, the entire southern part of the study area suffered from drought. During 2016, 2018, 2021, and 2022, the drought affected almost the entire study area, but with varying degrees of severity.

3.3. Temporal Variations in NDVI, Rainfall, and Temperature Anomalies

Except for the years 2016, 2020, 2021, and 2022, all of the other years displayed positive NDVI anomalies (Figure 6). Across the entire study duration, we noted three-year cycles of variation in the NDVI anomalies. The first three years (2011–2013) experienced a consistent rise in NDVI anomalies, peaking in 2013. This was followed by a decline from 2014 to 2016, culminating in negative values by 2016. A resurgence in positive NDVI anomalies occurred from 2017 to 2019, but this was again followed by a dip in 2020, hitting its lowest point in 2021. A generally consistent pattern between NDVI and rainfall anomalies was observed,

except for the years 2014 and 2021, which showed a divergent pattern. On the other hand, the pattern between temperature anomalies and NDVI anomalies was less predictable.

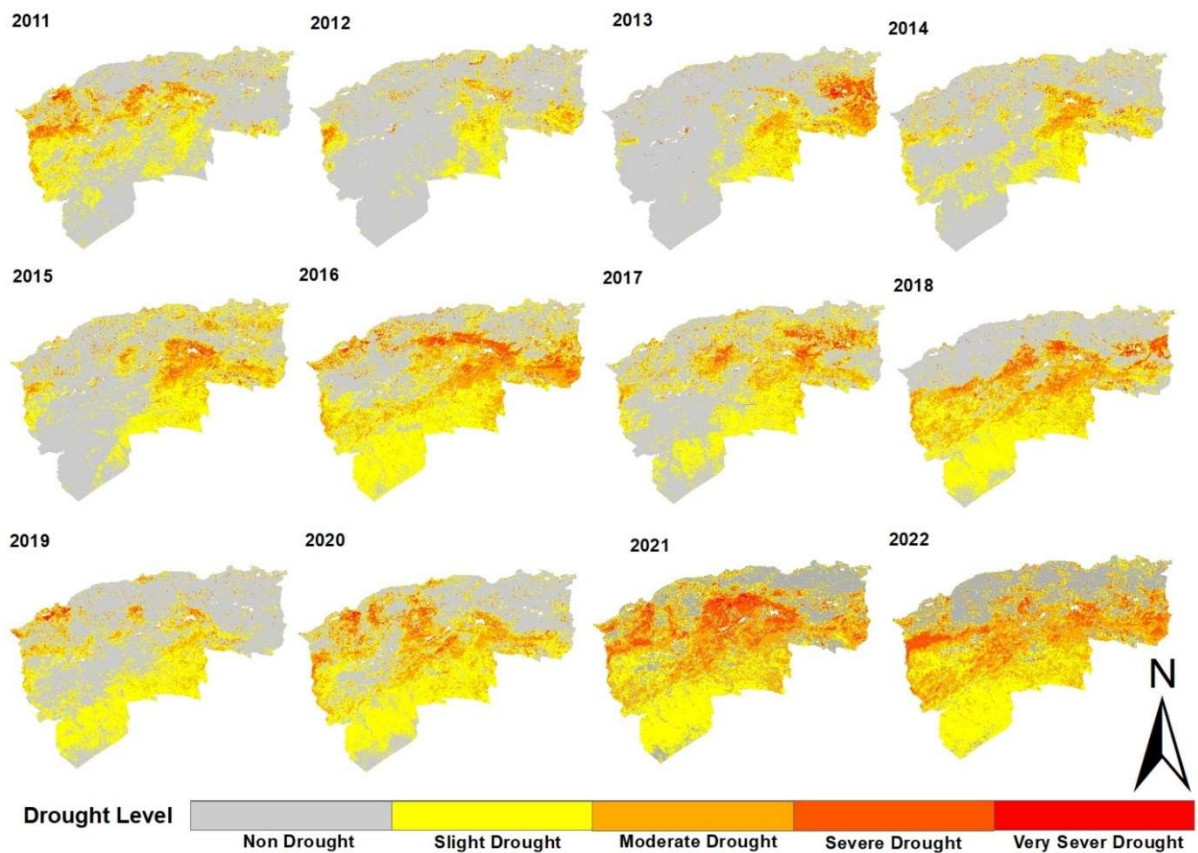


Figure 5. The spatial distribution of drought in northern Algeria from 2011 to 2022.

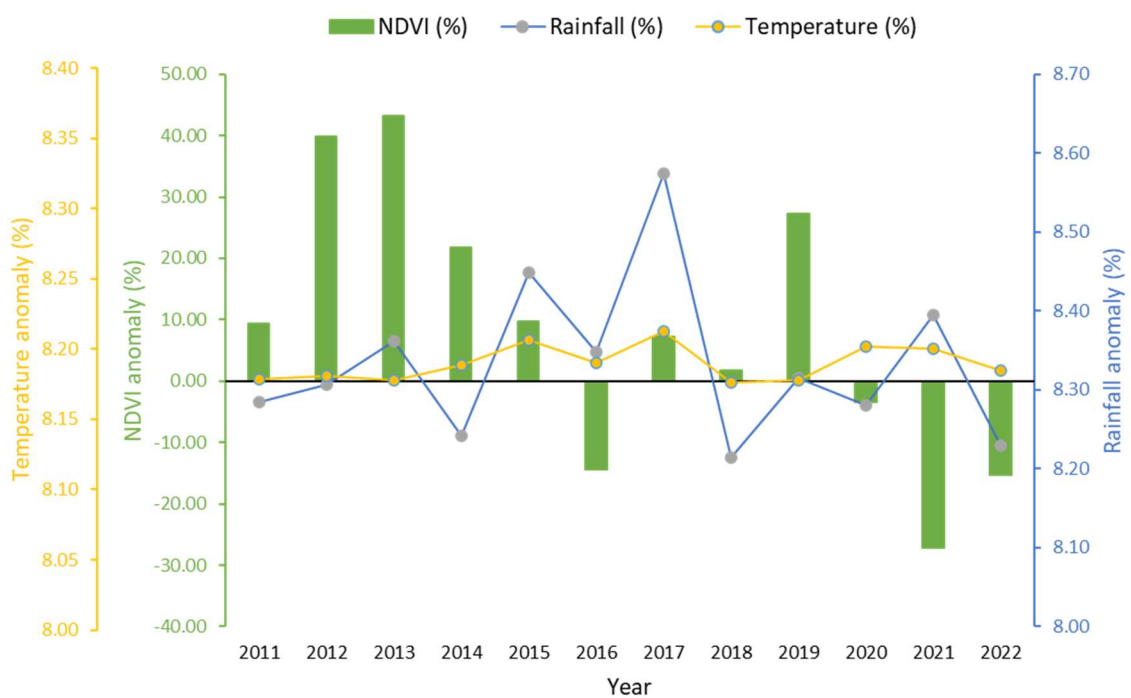


Figure 6. Seasonal variations in NDVI, rainfall, and temperature anomalies from 2011 to 2022.

3.4. Correlation of NDVI Anomaly with Rainfall and Temperature Anomalies

The Spearman correlation test was applied to quantify the strength and direction of the relationships between NDVI anomalies and rainfall and temperature anomalies. The findings indicated a statistically significant correlation ($p < 0.05$) between NDVI anomalies and climatic anomalies, although with varying degrees of strength across the different years (Figure 7). Specifically, the correlation between NDVI and rainfall was weak and predominantly positive, fluctuating between values of 0.10 and 0.37 over the study period. On the contrary, the correlation between NDVI and temperature anomalies was consistently negative throughout the years, with correlation coefficients typically ranging from negligible ($r_s = -0.01$) to moderate ($r_s = 0.47$).

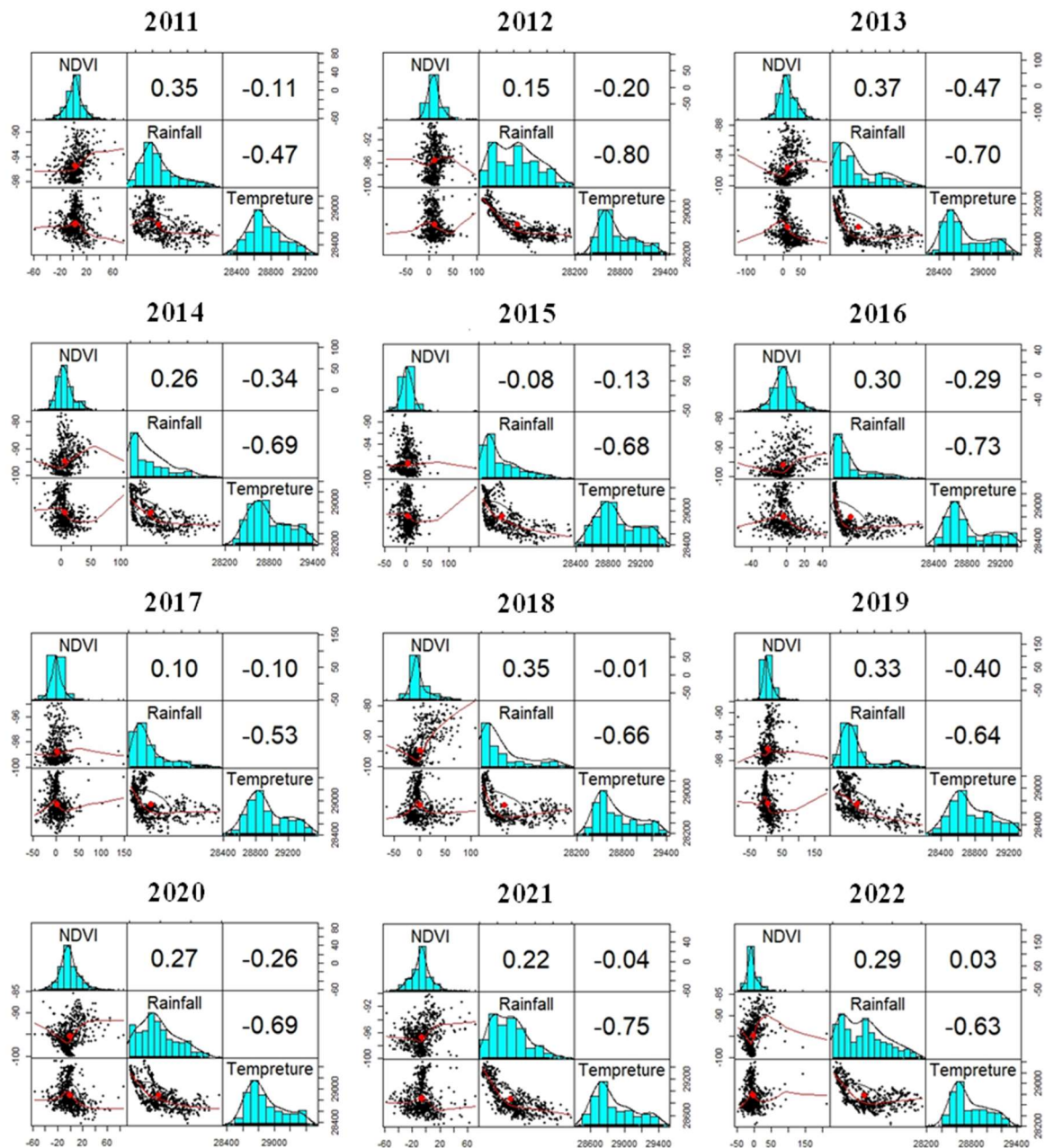


Figure 7. Spearman correlation coefficients (r_s) of NDVI, rainfall, and temperature anomalies from 2011 to 2022.

4. Discussion

4.1. Spatial and Temporal Patterns of Drought in Algeria during the Period 2011–2022

Our study revealed variable spatial and temporal patterns of drought during the study period. Despite fluctuations from year to year, there was an apparent pattern of increasing drought, with nearly 40% of the region experiencing overall drying conditions between 2011 and 2022, while certain areas did not show any obvious wetting pattern. The years 2012 and 2013 were the least drought-affected years, whereas 2016, 2021, and 2022 experienced the harshest drought conditions, affecting large areas with varying degrees of severity. These observations are in line with previous studies conducted in Algeria. For instance, [18] notably highlighted 2021 as part of a sustained dry spell in the country from 2012 to 2021. Similarly, [93] also classified 2020 as a distinctively dry year for the North African region, including Algeria. During these dry years, the median NDVI values consistently fell below 0.25, indicating widespread vegetation stress in the study area. While various parts of the region were affected, the southern section experienced the most significant impact, which is expected given the significant desertification in that area. However, even the northern coastal areas, which are usually vegetated, suffered from drought during extreme years like 2016. [73] corroborated our findings by identifying 2016 as a drought-prone year for Algeria. Interestingly, they also indicated that 2014 and 2015 were normal years, which is consistent with our results, showing these years as relatively minimally impacted by drought. This observation is further supported by [94], who also found no indications of drought characteristics in 2015. Such spatiotemporal patterns of drought are likely influenced by various factors, including climate variables, particularly rainfall and temperature, which are crucial for vegetation growth [95,96]. Consequently, we also investigated the relationship between vegetation and climate by utilizing the NDVI anomaly as an indicator of vegetation dynamics.

4.2. Relationship between NDVI and Climatic Factors

While rainfall and temperature are universally accepted as major elements influencing vegetation dynamics, differing conclusions have been drawn about the relative importance of these climatic variables in determining vegetation dynamics. For example, higher plant production is directly connected to high temperatures in the high-latitude region, while rainfall has a minimal impact [97]. Other studies, however, have found that vegetation productivity patterns were mainly driven by high rainfall [98–100]. In our study, while there is evidence to suggest the influence of rainfall on vegetation dynamics, such as the observed triennial fluctuations in the NDVI, the strength of this relationship considerably varied throughout the study period.

Specifically, our study identified a negligibly to moderately positive correlation between the NDVI anomaly and the rainfall anomaly, with correlation coefficients varying from $r_s = 0.10$ to 0.37, which aligns with previous research [24,100–103]. For example, [44] found a similar correlation coefficient range of 0.22 to 0.46. Similarly, [104] observed correlation coefficients ranging from 0.06 to 0.29, indicating a negligible to weak relationship between the NDVI and rainfall. Supported by these studies, our findings suggest a complex relationship between vegetation response and climatic factors. Vegetation health, as depicted by the NDVI, typically improves with increased rainfall, although this relationship varied from year to year. This variability was particularly evident in the correlation coefficient values for different years, indicating differing strengths of correlation between the NDVI and rainfall in different years.

We also observed that the correlation between the NDVI anomaly and the temperature anomaly was negative, mostly ranging from negligible and moderate correlations, implying that, during our study period, the vegetation health had a limited or barely noticeable correlation with temperature. Similarly, ref. [44] showed that temperature had a lesser impact on the NDVI anomaly compared to rainfall. However, other studies have shown that high temperatures inhibit vegetation growth, leading to a strong correlation between temperature and NDVI anomalies [105,106]. Given that northern Algeria covers a vast area,

the varying strengths of correlation observed between the NDVI and climate anomalies in different years are likely due to the spatial distribution of rainfall and temperature across the region, which can vary considerably. According to [25], rainfall variability tends to increase with an increase in longitude and a decrease in latitude. These disparities can lead to inconsistencies in the impact of rainfall and temperature on vegetation growth, as captured by NDVI.

4.3. Limitations and Future Research Opportunities

Our study underscores the complex interplay between climate conditions and vegetation dynamics in northern Algeria, an area known for its erratic weather patterns in terms of rainfall and temperature [25]. However, besides climate, other environmental factors, such as soil moisture, evapotranspiration rates, and local ecological dynamics, potentially play a crucial role in understanding the drought patterns in the region [107]. Consequently, there are opportunities for further investigation to explore the impacts of these environmental factors on present and future drought dynamics, as well as their correlation with the NDVI in northern Algeria.

Our analysis was conducted on a relatively shorter timescale, namely the annual timescale. As a result, we could not perform meaningful statistical tests for trends at such a short timescale. At this scale, the climatic variables generally exhibited weak correlations with the NDVI, albeit varying from year to year. More research is necessary to delve deeper into the relationship between the NDVI and climatic factors, examining it across different time scales, including daily and monthly scales [25,99,103].

This study has revealed complex and non-linear relationships between the NDVI and the climatic variables across most years. While the Spearman correlation was chosen over the Pearson correlation, due to its non-parametric nature, it too has limitations in capturing non-linear relationships [108]. Specifically, it relies on a monotonic relationship, albeit not strictly linear like the Pearson correlation [109]. Despite its limited ability to detect non-linear patterns, the Spearman correlation was still applicable in some years where a monotonic relationship was evident, with climate variables either positively or negatively changing with NDVI variations. Future investigations should explore alternative correlation methods, such as Kendall's tau [110] and distance correlation [111], which can capture non-linear relationships. These methods were not employed in this study due to their computational intensity, particularly with large datasets [109].

5. Conclusions

This study assessed the spatial and temporal patterns of drought and investigated the relationship between the growing season's NDVI anomaly and climate factors in northern Algeria from 2011 to 2022. The results have revealed that, in 2012 and 2013, northern Algeria experienced the least impact from drought, with over 70% of the study area experiencing non-drought conditions. Conversely, the years 2016, 2021, and 2022 were the most adversely affected by drought in the region. Throughout the study period, we observed recurring triennial fluctuations in the NDVI anomalies. The relationship between the NDVI anomaly and the climate factors varied across the years and was generally not strong. Therefore, we recommend further studies focusing on the link between the NDVI and climate factors, particularly over various time frames, such as daily and monthly periods. Overall, the MODIS-NDVI product provides an economically viable method for drought monitoring in data-limited areas such as Algeria, offering a potential alternative to climate-centric drought indices, which largely rely on sparse local rainfall stations.

Author Contributions: Conceptualization, R.B., G.S. and K.P.; methodology, R.B. and K.P.; software, R.B. and K.P.; validation, R.B., G.S., K.P. and F.H.; formal analysis, R.B. and K.P.; resources, F.H. and H.A.; data curation, R.B. and K.P.; writing—original draft preparation, R.B. and K.P.; writing—review and editing, R.B., K.P., G.S. and H.A.; supervision and funding acquisition G.S. All authors have read and agreed to the published version of the manuscript.

Funding: Project No. TKP2020-IKA-04 has been implemented with the support provided by the National Research, Development, and Innovation Fund of Hungary, financed under the 2020-4.1.1-TKP2020 funding scheme.

Data Availability Statement: The original contributions presented in the study are included in the article, further inquiries can be directed to the corresponding author.

Acknowledgments: The authors extend their heartfelt gratitude to The Department of Landscape Protection for generously providing the resources and support essential for the successful execution of this study. Additionally, we express our sincere appreciation for the support received from Project no. TKP2021-NKTA-32. This project was made possible through the funding provided by the National Research, Development, and Innovation Fund of Hungary, and we are deeply grateful for their contribution to our research endeavor. Furthermore, we would like to acknowledge the invaluable contributions of all authors involved in this work. Special thanks are extended to “Kwanale Phinzi” for his exceptional dedication and contributions to this study.

Conflicts of Interest: The authors declare no conflicts of interest.

References

1. Lee, R.H.; Navarro-Navarro, L.A.; Ley, A.L.; Hartfield, K.; Tolleson, D.R.; Scott, C.A. Spatio-temporal dynamics of climate change, land degradation, and water insecurity in an arid rangeland: The Río San Miguel watershed, Sonora, Mexico. *J. Arid. Environ.* **2021**, *193*, 104539. [[CrossRef](#)]
2. Sandford, R. The Human Face of Water Insecurity. In *Water Security in a New World*; Springer Nature: New York, NY, USA, 2017; pp. 1–24. [[CrossRef](#)]
3. Tsakiris, G.; Loukas, A.; Pangalou, D.; Vangelis, H.; Tigkas, D.; Rossi, G.; Cancelliere, A. Chapter 7. Drought Characterization. *Drought Manag. Guidel. Tech. Annex.* **2007**, *58*, 85–102.
4. Intergovernmental Panel on Climate Change (IPCC). Desertification. In *Climate Change and Land: IPCC Special Report on Climate Change, Desertification, Land Degradation, Sustainable Land Management, Food Security, and Greenhouse Gas Fluxes in Terrestrial Ecosystems*; Cambridge University Press: Cambridge, UK, 2019; pp. 66–70. [[CrossRef](#)]
5. Chakilu, G.G.; Sándor, S.; Zoltán, T.; Phinzi, K. Climate change and the response of streamflow of watersheds under the high emission scenario in Lake Tana sub-basin, upper Blue Nile basin, Ethiopia. *J. Hydrol. Reg. Stud.* **2022**, *42*, 101175. [[CrossRef](#)]
6. Jenkins, K.; Dobson, B.; Decker, C.; Hall, J.W. An Integrated Framework for Risk-Based Analysis of Economic Impacts of Drought and Water Scarcity in England and Wales. *Water Resour. Res.* **2021**, *57*, e2020WR027715. [[CrossRef](#)]
7. Haile, G.G.; Tang, Q.; Li, W.; Liu, X.; Zhang, X. Drought: Progress in broadening its understanding. *WIREs Water* **2019**, *7*, e1407. [[CrossRef](#)]
8. Mitra, S.; Srivastava, P. Comprehensive Drought Assessment Tool for Coastal Areas, Bays, and Estuaries: Development of a Coastal Drought Index. *J. Hydrol. Eng.* **2021**, *26*, 04020055.
9. Wilhite, D.A. Chapter 1 Drought as a Natural Hazard: Concepts and Definitions. In *Droughts: A Global Assessment*; Routledge: London, UK, 2000.
10. Dai, A. Drought under global warming: A review. *Wiley Interdiscip. Rev. Clim. Change* **2011**, *2*, 45–65, Erratum in *Wiley Interdiscip. Rev. Clim. Change* **2012**, *3*, 617.
11. Zhong, R.; Chen, X.; Lai, C.; Wang, Z.; Lian, Y.; Yu, H.; Wu, X. Drought monitoring utility of satellite-based precipitation products across mainland China. *J. Hydrol.* **2018**, *568*, 343–359. [[CrossRef](#)]
12. Mishra, A.K.; Singh, V.P. A review of drought concepts. *J. Hydrol.* **2010**, *391*, 202–216. [[CrossRef](#)]
13. Sun, Y.; Solomon, S.; Dai, A.; Portmann, R.W. How Often Does It Rain? *J. Clim.* **2006**, *19*, 916–934. [[CrossRef](#)]
14. Wilhite, D.A.; Glantz, M.H. Understanding: The Drought Phenomenon: The Role of Definitions. *Water Int.* **1985**, *10*, 111–120. [[CrossRef](#)]
15. Lam, M.R.; Matanó, A.; Van Loon, A.F.; Odongo, R.A.; Teklesadik, A.D.; Wamucii, C.N.; Homberg, M.J.C.v.D.; Waruru, S.; Teuling, A.J. Linking reported drought impacts with drought indices, water scarcity and aridity: The case of Kenya. *Nat. Hazards Earth Syst. Sci.* **2023**, *23*, 2915–2936. [[CrossRef](#)]
16. Ahmadalipour, A.; Moradkhani, H. Multi-dimensional assessment of drought vulnerability in Africa: 1960–2100. *Sci. Total. Environ.* **2018**, *644*, 520–535. [[CrossRef](#)] [[PubMed](#)]
17. Lyon, B. Seasonal Drought in the Greater Horn of Africa and Its Recent Increase during the March–May Long Rains. *J. Clim.* **2014**, *27*, 7953–7975. [[CrossRef](#)]
18. Derdous, O.; Bouamrane, A.; Mrad, D. Spatiotemporal analysis of meteorological drought in a Mediterranean dry land: Case of the Cheliff basin–Algeria. *Model. Earth Syst. Environ.* **2020**, *7*, 135–143. [[CrossRef](#)]
19. Gader, K.; Gara, A.; Vanclooster, M.; Khlifi, S.; Slimani, M. Drought assessment in a south Mediterranean transboundary catchment. *Hydrol. Sci. J.* **2020**, *65*, 1300–1315. [[CrossRef](#)]

20. Tramblay, Y.; Koutroulis, A.; Samaniego, L.; Vicente-Serrano, S.M.; Volaire, F.; Boone, A.; Le Page, M.; Llasat, M.C.; Albergel, C.; Burak, S.; et al. Challenges for drought assessment in the Mediterranean region under future climate scenarios. *Earth-Sci. Rev.* **2020**, *210*, 103348. [[CrossRef](#)]
21. Giorgi, F.; Lionello, P. Climate change projections for the Mediterranean region. *Glob. Planet. Chang.* **2008**, *63*, 90–104. [[CrossRef](#)]
22. Collins, M.; Knutti, R. *Long-Term Climate Change: Projections, Commitments and Irreversibility. Climate Change 2013 the Physical Science Basis: Working Group I Contribution to the Fifth Assessment Report of the Intergovernmental Panel on Climate Change*; Cambridge University Press: Cambridge, UK, 2013; pp. 1029–1136. [[CrossRef](#)]
23. Reay, D.; Sabine, C.; Smith, P.; Hymus, G. *Intergovernmental Panel on Climate Change. Fourth Assessment Report*; Cambridge University Press: Cambridge, UK; Geneva, Switzerland, 2007; Available online: <https://www.ipcc.ch> (accessed on 11 April 2007). [[CrossRef](#)]
24. Elair, C.; Chaham, K.R.; Hadri, A. Assessment of drought variability in the Marrakech-Safi region (Morocco) at different time scales using GIS and remote sensing. *Water Supply* **2023**, *23*, 4592–4624. [[CrossRef](#)]
25. Meddi, H.; Meddi, M.; Assani, A.A. Study of Drought in Seven Algerian Plains. *Arab. J. Sci. Eng.* **2013**, *39*, 339–359. [[CrossRef](#)]
26. Meddi, M.; Hubert, P. *Impact de la Modification du Régime Pluviométrique sur les Ressources en eau du Nord-Ouest de L’algérie*; IAHS publication: Wallingford, UK, 2003; pp. 229–235.
27. Mellak, S.; Souag-Gamane, D. Spatio-temporal analysis of maximum drought severity using Copulas in Northern Algeria. *J. Water Clim. Chang.* **2020**, *11*, 68–84. [[CrossRef](#)]
28. Nouaceur, Z.; Laignel, B.; Turki, I. Changements climatiques au Maghreb: Vers des conditions plus humides et plus chaudes sur le littoral algérien? *Physio-Géo. Géographie Phys. Environ.* **2013**, *7*, 307–323. [[CrossRef](#)]
29. Salamani, M.; Hirche, A.; Boughani, A.; Alia, E.; Ezzouar, B.; Alger, A. Évolution de la pluviosité annuelle dans quelques stations arides algériennes. *Sécheresse* **2007**, *18*, 314–320.
30. Seltzer, P.; Lasserre, A.; Grandjean, A.; Auberty, R.; Fourey, A. *Le Climat de l’Algérie. par P. Seltzer... Étude publiée avec le concours de A. Lasserre... Mlle A. Grandjean, R. Au-berty et A. Fourey. [Préface de P. Queney.]*; Impr. La Typo-Litho et de J. Carbonel réunies: Dely Ibrahim, Algeria, 1946.
31. Fellag, M.; Achite, M.; Walega, A. Spatial-temporal characterization of meteorological drought using the Standardized precipitation index. Case study in Algeria. *Acta Sci. Polonorum. Form. Circumiectus* **2021**, *20*, 19–31. [[CrossRef](#)]
32. AghaKouchak, A.; Farahmand, A.; Melton, F.S.; Teixeira, J.; Anderson, M.C.; Wardlow, B.D.; Hain, C.R. Remote sensing of drought: Progress, challenges and opportunities. *Rev. Geophys.* **2015**, *53*, 452–480. [[CrossRef](#)]
33. Palmer, W.C. *Meteorological Drought*; Department of Commerce, Weather Bureau: Washington, DC, USA, 1965.
34. Vicente-Serrano, S.M.; Beguería, S.; López-Moreno, J.I. A Multiscalar Drought Index Sensitive to Global Warming: The Standardized Precipitation Evapotranspiration Index. *J. Clim.* **2010**, *23*, 1696–1718. [[CrossRef](#)]
35. Mckee, T.B.; Doesken, N.J.; Kleist, J. The relationship of drought frequency and duration to time scales. In Proceedings of the Eighth Conference on Applied Climatology, Anaheim, CA, USA, 17–22 January 1993; pp. 17–22.
36. Bijaber, N.; El Hadani, D.; Saidi, M.; Svoboda, M.D.; Wardlow, B.D.; Hain, C.R.; Poulsen, C.C.; Yesséf, M.; Rochdi, A. Developing a Remotely Sensed Drought Monitoring Indicator for Morocco. *Geosciences* **2018**, *8*, 55. [[CrossRef](#)]
37. Derradji, T.; Belksier, M.-S.; Bouznad, I.-E.; Zebba, R.; Bengusmia, D.; Guastaldi, E. Spatio-temporal drought monitoring and detection of the areas most vulnerable to drought risk in Mediterranean region, based on remote sensing data (Northeastern Algeria). *Arab. J. Geosci.* **2022**, *16*, 1. [[CrossRef](#)]
38. Hadri, A.; El, M.; Saidi, M.; Boudhar, A. Multiscale drought monitoring and comparison using remote sensing in a Mediterranean arid region: A case study from west-central Morocco. *Arab. J. Geosci.* **2021**, *14*, 118.
39. Ntale, H.K.; Gan, T.Y. Drought indices and their application to East Africa. *Int. J. Clim.* **2003**, *23*, 1335–1357. [[CrossRef](#)]
40. Aksoy, S.; Gorucu, O.; Sertel, E. 2019 the Eighth International Conference on Agro-Geoinformatics. In Proceedings of the 8th International Conference on Agro-Geoinformatics (Agro-Geoinformatics), Istanbul, Turkey, 16–19 July 2019.
41. Su, B.; Huang, J.; Fischer, T.; Wang, Y.; Kundzewicz, Z.W.; Zhai, J.; Sun, H.; Wang, A.; Zeng, X.; Wang, G.; et al. Drought losses in China might double between the 1.5 °C and 2.0 °C warming. *Proc. Natl. Acad. Sci. USA* **2018**, *115*, 10600–10605. [[CrossRef](#)] [[PubMed](#)]
42. Sun, H.; Xu, Q.; Wang, Y.; Zhao, Z.; Zhang, X.; Liu, H.; Gao, J. Agricultural drought dynamics in China during 1982–2020: A depiction with satellite remotely sensed soil moisture. *GIScience Remote Sens.* **2023**, *60*, 2257469. [[CrossRef](#)]
43. Touhami, I.; Moutahir, H.; Assoul, D.; Bergaoui, K.; Aouinti, H.; Bellot, J.; Andreu, J.M. Multi-year monitoring land surface phenology in relation to climatic variables using MODIS-NDVI time-series in Mediterranean forest, Northeast Tunisia. *Acta Oecologica* **2021**, *114*, 103804. [[CrossRef](#)]
44. Nanzad, L.; Zhang, J.; Tuvdendorj, B.; Nabil, M.; Zhang, S.; Bai, Y. NDVI anomaly for drought monitoring and its correlation with climate factors over Mongolia from 2000 to 2016. *J. Arid. Environ.* **2019**, *164*, 69–77. [[CrossRef](#)]
45. Easterling, D.R. Global Data Sets for Analysis of Climate Extremes. In *Extremes in a Changing Climate: Detection, Analysis and Uncertainty*; Springer: Dordrecht, The Netherlands, 2013; pp. 347–361. [[CrossRef](#)]
46. AghaKouchak, A.; Nakhjiri, N. A near real-time satellite-based global drought climate data record. *Environ. Res. Lett.* **2012**, *7*, 044037. [[CrossRef](#)]
47. Hateffard, F.; Szatmári, G.; Novák, T.J. Applicability of machine learning models for predicting soil organic carbon content and bulk density under different soil conditions. *Soil Sci. Ann.* **2023**, *74*, 165879. [[CrossRef](#)]

48. Krishna, T.M.; Ravikumar, G.; Krishnaveni, M. Remote sensing based agricultural drought assessment in Palar basin of Tamil Nadu state, India. *J. Indian Soc. Remote Sens.* **2009**, *37*, 9–20. [[CrossRef](#)]
49. Rhee, J.; Im, J.; Carbone, G.J. Monitoring agricultural drought for arid and humid regions using multi-sensor remote sensing data. *Remote Sens. Environ.* **2010**, *114*, 2875–2887. [[CrossRef](#)]
50. Sandeep, P.; Reddy, G.O.; Jegankumar, R.; Kumar, K.A. Monitoring of agricultural drought in semi-arid ecosystem of Peninsular India through indices derived from time-series CHIRPS and MODIS datasets. *Ecol. Indic.* **2020**, *121*, 107033. [[CrossRef](#)]
51. Rouse, J.W.; Haas, R.H.; Schell, J.A.; Deering, D.W. Monitoring Vegetation Systems in the Great Plains with ERTS. Third ERTS-1 Symposium NASA. *NASA Spec. Publ.* **1974**, *351*, 309–317.
52. Kogan, F. Application of vegetation index and brightness temperature for drought detection. *Adv. Space Res.* **1995**, *15*, 91–100. [[CrossRef](#)]
53. Lu, J.; Carbone, G.J.; Gao, P. Mapping the agricultural drought based on the long-term AVHRR NDVI and North American Regional Reanalysis (NARR) in the United States, 1981–2013. *Appl. Geogr.* **2019**, *104*, 10–20. [[CrossRef](#)]
54. Singh, R.P.; Roy, S.; Kogan, F. Vegetation and temperature condition indices from NOAA AVHRR data for drought monitoring over India. *Int. J. Remote Sens.* **2003**, *24*, 4393–4402. [[CrossRef](#)]
55. Wang, H.; Chen, A.; Wang, Q.; He, B. Drought dynamics and impacts on vegetation in China from 1982 to 2011. *Ecol. Eng.* **2015**, *75*, 303–307. [[CrossRef](#)]
56. Peters, A.J.; Rundquist, D.C.; Wilhite, D.A. Satellite detection of the geographic core of the 1988 Nebraska drought. *Agric. For. Meteorol.* **1991**, *57*, 35–47. [[CrossRef](#)]
57. Buras, A.; Rammig, A.; Zang, C.S. Quantifying impacts of the 2018 drought on European ecosystems in comparison to 2003. *Biogeosciences* **2020**, *17*, 1655–1672. [[CrossRef](#)]
58. Van Hoek, M.; Jia, L.; Zhou, J.; Zheng, C.; Menenti, M. Early Drought Detection by Spectral Analysis of Satellite Time Series of Precipitation and Normalized Difference Vegetation Index (NDVI). *Remote Sens.* **2016**, *8*, 422. [[CrossRef](#)]
59. Ji, L.; Peters, A.J. Assessing vegetation response to drought in the northern Great Plains using vegetation and drought indices. *Remote Sens. Environ.* **2003**, *87*, 85–98. [[CrossRef](#)]
60. Li, R.; Tsunekawa, A.; Tsubo, M. Index-based assessment of agricultural drought in a semi-arid region of Inner Mongolia, China. *J. Arid. Land* **2013**, *6*, 3–15. [[CrossRef](#)]
61. Wang, J.; Price, K.P.; Rich, P.M. Spatial patterns of NDVI in response to precipitation and temperature in the central Great Plains. *Int. J. Remote Sens.* **2001**, *22*, 3827–3844. [[CrossRef](#)]
62. Anyamba, A.; Wang, J.; Liu, W.T. NDVI anomaly patterns over Africa during the 1997/98 ENSO warm event. *Int. J. Remote Sens.* **2001**, *22*, 1847–1859. [[CrossRef](#)]
63. Liu, W.T.; Juárez, R.N. ENSO drought onset prediction in northeast Brazil using NDVI. *Int. J. Remote Sens.* **2010**, *22*, 3483–3501. [[CrossRef](#)]
64. Kamble, M.V.; Ghosh, K.; Rajeevan, M.; Samui, R.P. Drought monitoring over India through Normalized Difference Vegetation Index (NDVI). *Mausam* **2010**, *61*, 537–546. [[CrossRef](#)]
65. Achour, K.; Meddi, M.; Zeroual, A.; Bouabdelli, S.; Maccioni, P.; Moramarco, T. Spatio-temporal analysis and forecasting of drought in the plains of northwestern Algeria using the standardized precipitation index. *J. Earth Syst. Sci.* **2020**, *129*, 42. [[CrossRef](#)]
66. Bentchakal, M.; Medjerab, A.; Chibane, B.; Rahmani, S.E.A. Meteorological drought and remote sensing data: An approach to assess fire risks in the Algerian forest. *Model. Earth Syst. Environ.* **2021**, *8*, 3847–3858. [[CrossRef](#)]
67. Berhail, S.; Tourki, M.; Merrouche, I.; Bendekiche, H. Geo-statistical assessment of meteorological drought in the context of climate change: Case of the Macta basin (Northwest of Algeria). *Model. Earth Syst. Environ.* **2021**, *8*, 81–101.
68. Elouissi, A.; Benzater, B.; Dabanli, I.; Habi, M.; Harizia, A.; Hamimed, A. Drought investigation and trend assessment in Macta watershed (Algeria) by SPI and ITA methodology. *Arab. J. Geosci.* **2021**, *14*, 1329. [[CrossRef](#)]
69. Frih, B.; Oulmi, A.; Guendouz, A. Study of Drought Tolerance of Some Durum Wheat (*Triticum durum* Desf.) Genotypes Growing under Semi-arid Conditions in Algeria. *Int. J. Bio-resource Stress Manag.* **2021**, *12*, 137–141. [[CrossRef](#)]
70. Habibi, B.; Meddi, M. Meteorological drought hazard analysis of wheat production in the semi-arid basin of Cheliff–Zahrez Nord, Algeria. *Arab. J. Geosci.* **2021**, *14*, 1045. [[CrossRef](#)]
71. Hallouz, F.; Meddi, M.; Mahé, G.; Rahmani, S.A.; Karahacane, H.; Brahimi, S. Analysis of meteorological drought sequences at various timescales in semi-arid climate: Case of the Cheliff watershed (northwest of Algeria). *Arab. J. Geosci.* **2020**, *13*, 280. [[CrossRef](#)]
72. Khezazna, A.; Amarchi, H.; Derdous, O.; Bousakhria, F. Drought monitoring in the Seybouse basin (Algeria) over the last decades. *J. Water Land Dev.* **2017**, *33*, 79–88. [[CrossRef](#)]
73. HENCHIRI, M.; LIU, Q.; ESSIFI, B.; JAVED, T.; ZHANG, S.; BAI, Y.; ZHANG, J. Spatio-Temporal Patterns of Drought and Impact on Vegetation in North and West Africa Based on Multi-Satellite Data. *Remote Sens.* **2020**, *12*, 3869. [[CrossRef](#)]
74. Habibi, B.; Meddi, M.; Emre, T.; Boucefiane, A.; Rahmouni, A. Drought assessment and characterization using SPI, EDI and DEPI indices in northern Algeria. *Nat. Hazards* **2024**, *120*, 5201–5231. [[CrossRef](#)]
75. Derdour, A.; Bouarfa, S.; Kaid, N.; Baili, J.; Al-Bahrani, M.; Menni, Y.; Ahmad, H. Assessment of the impacts of climate change on drought in an arid area using drought indices and Landsat remote sensing data. *Int. J. Low-Carbon Technol.* **2022**, *17*, 1459–1469. [[CrossRef](#)]

76. Thiemig, V.; Rojas, R.; Zambrano-Bigiarini, M.; Levizzani, V.; De Roo, A. Validation of Satellite-Based Precipitation Products over Sparsely Gauged African River Basins. *J. Hydrometeorol.* **2012**, *13*, 1760–1783. [[CrossRef](#)]
77. Boudiaf, B.; Şen, Z.; Boutaghane, H. Climate change impact on rainfall in north-eastern Algeria using innovative trend analyses (ITA). *Arab. J. Geosci.* **2021**, *14*, 511. [[CrossRef](#)]
78. Jean-Pierre, L.; Philippe, G.; Mohamed, A.; Abdelmatif, D.; Larbi, B. Climate evolution and possible effects on surface water resources of North Algeria. *Curr. Sci.* **2010**, *98*, 1056–1062.
79. Hersbach, H.; Bell, B.; Berrisford, P.; Biavati, G.; Horányi, A.; Muñoz Sabater, J.; Nicolas, J.; Peubey, C.; Radu, R.; Rozum, I.; et al. ERA5 monthly averaged data on single levels from 1940 to present. 2023. Available online: https://scholar.google.com/citations?view_op=view_citation&hl=fr&user=TOdNTtAAAAAJ&cstart=20&pagesize=80&sortby=pubdate&citation_for_view=TOdNTtAAAAAJ:q3oQSFYPqjQC (accessed on 29 April 2024).
80. Muñoz Sabater, J. ERA5-Land hourly data from 1950 to present. Copernicus Climate Change Service (C3S) Climate Data Store (CDS) 2019. Available online: <https://cds.climate.copernicus.eu/cdsapp#!/dataset/10.24381/cds.e2161bac?tab=overview> (accessed on 28 April 2024).
81. Kusch, E.; Davy, R. KrigR—A tool for downloading and statistically downscaling climate reanalysis data. *Environ. Res. Lett.* **2022**, *17*, 024005. [[CrossRef](#)]
82. Tucker, C.J. Red and Photographic Infrared linear Combinations for Monitoring Vegetation. *Remote Sens. Environ.* **1979**, *8*, 127–150. [[CrossRef](#)]
83. Anyamba, A.; Tucker, C.J. Historical Perspectives on AVHRR NDVI and Vegetation Drought Monitoring. In *Remote Sensing of Drought*, 1st ed.; CRC Press: Boca Raton, FL, USA, 2012. [[CrossRef](#)]
84. Vaani, N.; Porchelvan, P. Assessment of long term agricultural drought in Tamilnadu, India using NDVI anomaly. *Disaster Adv.* **2017**, *10*, 1–10.
85. Arguez, A.; Vose, R.S. The Definition of the Standard WMO Climate Normal: The Key to Deriving Alternative Climate Normals. *Bull. Am. Meteorol. Soc.* **2011**, *92*, 699–704. [[CrossRef](#)]
86. Legesse, G.; Suryabhagavan, K.V. Remote sensing and GIS based agricultural drought assessment in East Shewa zone, Ethiopia. *Trop. Ecol.* **2014**, *55*, 349–363.
87. Kourouma, J.M.; Eze, E.; Negash, E.; Phiri, D.; Vinya, R.; Girma, A.; Zenebe, A. Assessing the spatio-temporal variability of NDVI and VCI as indices of crops productivity in Ethiopia: A remote sensing approach. *Geomat. Nat. Hazards Risk* **2021**, *12*, 2880–2903. [[CrossRef](#)]
88. Wickham, H. *ggplot2 Elegant Graphics for Data Analysis*; Springer: Berlin/Heidelberg, Germany, 2016.
89. Xiao, C.; Ye, J.; Esteves, R.M.; Rong, C. Using Spearman’s correlation coefficients for exploratory data analysis on big dataset. *Concurr. Comput. Pract. Exp.* **2015**, *28*, 3866–3878. [[CrossRef](#)]
90. Janse, R.J.; Hoekstra, T.; Jager, K.J.; Zoccali, C.; Tripepi, G.; Dekker, F.W.; van Diepen, M. Conducting correlation analysis: Important limitations and pitfalls. *Clin. Kidney J.* **2021**, *14*, 2332–2337. [[CrossRef](#)] [[PubMed](#)]
91. R Core Team. *R: A language and environment for statistical Computing*; R Foundation for Statistical Computing: Vienna, Austria, 2021.
92. Schober, P.; Boer, C.; Schwarte, L.A. Correlation Coefficients: Appropriate Use and Interpretation. *Anesth. Analg.* **2018**, *126*, 1763–1768. [[CrossRef](#)] [[PubMed](#)]
93. Thi, N.Q.; Govind, A.; Le, M.-H.; Linh, N.T.; Anh, T.T.M.; Hai, N.K.; Ha, T.V. Spatiotemporal characterization of droughts and vegetation response in Northwest Africa from 1981 to 2020. *Egypt. J. Remote Sens. Space Sci.* **2023**, *26*, 393–401. [[CrossRef](#)]
94. Abbes, M.; Hamimed, A.; Lafrid, A.; Mahi, H.; Nehal, L. Use of high spatial resolution satellite data for monitoring and characterization of drought conditions in the Northwestern Algeria. *Min. Sci.* **2018**, *25*, 85–113. [[CrossRef](#)]
95. De Jong, R.; Verbesselt, J.; Zeileis, A.; Schaepman, M.E. Shifts in Global Vegetation Activity Trends. *Remote Sens.* **2013**, *5*, 1117–1133. [[CrossRef](#)]
96. Zhou, L.; Tucker, C.J.; Kaufmann, R.K.; Slayback, D.; Shabanov, N.V.; Myneni, R.B. Variations in Northern Vegetation Activity Inferred from Satellite Data of Vegetation Index during 1981 to 1999. *J. Geophys. Res. Atmos.* **2001**, *106*, 20069–20083. [[CrossRef](#)]
97. Tucker, C.J.; Slayback, D.A.; Pinzon, J.E.; Los, S.O.; Myneni, R.B.; Taylor, M.G. Higher northern latitude normalized difference vegetation index and growing season trends from 1982 to 1999. *Int. J. Biometeorol.* **2001**, *45*, 184–190. [[CrossRef](#)]
98. Piao, S.; Fang, J.; Zhou, L.; Zhu, B.; Tan, K.; Tao, S. Changes in vegetation net primary productivity from 1982 to 1999 in China. *Glob. Biogeochem. Cycles* **2005**, *19*. [[CrossRef](#)]
99. Ghabi, M.; Khelifa, D.; Benmansour, N. Exploring Relationships Between Precipitation (Trmm) and Vegetation Dynamics (Case Study of Sidi Bel Abbes). In Proceedings of the 7th International Conference on Cartography and GIS, Sozopol, Bulgaria, 18–23 June 2018.
100. Fayeche, D.; Tarhouni, J. Climate variability and its effect on normalized difference vegetation index (NDVI) using remote sensing in semi-arid area. *Model. Earth Syst. Environ.* **2020**, *7*, 1667–1682. [[CrossRef](#)]
101. Brumbaugh, F. What is an I.Q.? *J. Exp. Educ.* **1955**, *23*, 359–363. [[CrossRef](#)]
102. Jiang, Z.; Huete, A.R.; Didan, K.; Miura, T. Development of a two-band enhanced vegetation index without a blue band. *Remote Sens. Environ.* **2008**, *112*, 3833–3845. [[CrossRef](#)]
103. Piao, S.; Mohammat, A.; Fang, J.; Cai, Q.; Feng, J. NDVI-based increase in growth of temperate grasslands and its responses to climate changes in China. *Glob. Environ. Chang.* **2006**, *16*, 340–348. [[CrossRef](#)]

104. Hou, W.; Gao, J.; Wu, S.; Dai, E. Interannual Variations in Growing-Season NDVI and Its Correlation with Climate Variables in the Southwestern Karst Region of China. *Remote Sens.* **2015**, *7*, 11105–11124. [[CrossRef](#)]
105. Chakraborty, T.; Hsu, A.; Many, D.; Sheriff, G. A spatially explicit surface urban heat island database for the United States: Characterization, uncertainties, and possible applications. *ISPRS J. Photogramm. Remote Sens.* **2020**, *168*, 74–88. [[CrossRef](#)]
106. Wang, C.; Wang, J.; Naudiyal, N.; Wu, N.; Cui, X.; Wei, Y.; Chen, Q. Multiple Effects of Topographic Factors on Spatio-Temporal Variations of Vegetation Patterns in the Three Parallel Rivers Region, Southeast Qinghai-Tibet Plateau. *Remote Sens.* **2021**, *14*, 151. [[CrossRef](#)]
107. Eklundh, L.; Jönsson, P. *TIMESAT 3.3 Software Manual*; Lund University: Lund, Sweden, 2017; pp. 1–92.
108. Armstrong, R.A. Should Pearson’s correlation coefficient be avoided? *Ophthalmic Physiol. Opt.* **2019**, *39*, 316–327. [[CrossRef](#)]
109. Hastie, T.; Friedman, J.; Tibshirani, R. *The Elements of Statistical Learning*; Springer Series in Statistics; Springer: New York, NY, USA, 2001. [[CrossRef](#)]
110. Kendall, M.G. A New Measure of Rank Correlation. *Biometrika* **1938**, *30*, 81. [[CrossRef](#)]
111. Székely, G.J.; Rizzo, M.L. Brownian Distance Covariance. *Ann. Appl. Stat.* **2009**, *3*, 1236–1265. [[CrossRef](#)] [[PubMed](#)]

Disclaimer/Publisher’s Note: The statements, opinions and data contained in all publications are solely those of the individual author(s) and contributor(s) and not of MDPI and/or the editor(s). MDPI and/or the editor(s) disclaim responsibility for any injury to people or property resulting from any ideas, methods, instructions or products referred to in the content.